Macromolecules
ARTICLE

Macromolecules **2010**, *43*, 3415–3421 **3415**
DOI: 10.1021/ma902484d

Immobilized Polymer Layers on Spherical Nanoparticles

Shane E. Harton,[†] Sanat K. Kumar,*[,†] Hoichang Yang,[‡] Tadanori Koga,[§] Kyle Hicks,[∥] HyungKi Lee,[∥] Jovan Mijovic,[∥] Ming Liu,[⊥] Richard S. Vallery,[⊥] and David W. Gidley*[,⊥]

[†]*Department of Chemical Engineering, Columbia University, New York, New York,* [‡]*Rensselaer Nanotechnology Institute, Rensselaer Polytechnic University, Troy, New York,* [§]*Chemical and Molecular Engineering Program, Department of Materials Science and Engineering, Stony Brook University, Stony Brook, New York,* [∥]*Othmer-Jacobs Department of Chemical and Biological Engineering, Polytechnic Institute of New York University, Brooklyn, New York, and* [⊥]*Department of Physics, University of Michigan, Ann Arbor, Michigan*

Received November 9, 2009; Revised Manuscript Received February 10, 2010

ABSTRACT: Polymer properties, such as their mechanical strength, barrier properties, and dielectric response, can be dramatically improved by the addition of nanoparticles. This improvement is thought to be because the surface area per unit mass of particles increases with decreasing particle size, R, as $1/R$. This favorable effect has to be reconciled with the expectation that at small enough R the nanoparticles must behave akin to a solvent and cause a deterioration of properties. How does this transition in behavior from large solutes to the solvent limit occur? We conjecture that for small enough particles the layer of polymer affected by the particles ("bound" polymer layer) must be much smaller than that for large particles: the favorable effect of increasing particle surface area can thus be overcome and lead to the small solvent limit with unfavorable mechanical properties, for example. To substantiate this picture requires that we measure and compare the "bound polymer layer" formed on nanoparticles with those near large particles with equivalent chemistry. We have implemented a novel strategy to obtain uniform nanoparticle dispersion in polymers, a problem for many previous works. Then, by combining theory and a suite of experimental techniques, including differential scanning calorimetry and positron annihilation lifetime spectroscopy, we show that the immobilized poly(2-vinylpyridine) layer near 15 nm diameter silica particles (~1 nm) is considerably thinner than that at flat silica surfaces (~4 to 5 nm), which is the limit of an infinitely large particle. We have also determined that the changes in the polymer's glass-transition temperature due to the presence of this strongly interacting surface are very small in both well-dispersed nanocomposites and thin films (< 100 nm). Similarly, the polymer's fragility, as determined by dielectric spectroscopy, is also found to be little affected in the nanocomposites relative to the pure polymer. While a systematic study of the dependence of the bound polymer layer thickness on particle size remains an outstanding challenge, this first study provides conclusive evidence for the hypothesis that the bound polymer layer can be significantly smaller around nanoparticles than at chemically similar flat surfaces.

1. Introduction

Polymer nanocomposites have gained considerable interest in recent years. Because of their high surface-area-to-volume ratio, incorporating nanoparticles within a polymer matrix can greatly enhance properties such as mechanical strength or electrical conductivity.[1] The favorable effect of adding particles to a polymer stems from the fact that the surface area per unit mass of particles increases as $1/R$, where R is the characteristic dimension of the isotropic filler particle. In contrast, very small particles (< 1 to 2 nm) can actually plasticize the polymer matrix,[2] resulting in diminished properties and performance. We conjecture that this deterioration of properties for the smallest particles occurs because the bound layer of polymer formed near surfaces decreases sharply for the smallest nanoparticles (relative to their planar analogs). Indeed, there has been considerable interest in the "immobilized" polymer layer that forms spontaneously at an attractive planar surface[3−7] because it is postulated to control the dynamics of technologically relevant thin polymer films, for example, in lithography. Similarly, nanoparticles in filled polymers can be dynamically coupled through the bridging of adsorbed layers on adjacent particles.[5,8−12] When such coupled structures percolate, several properties can be significantly improved, making nanocomposites attractive for use in applications such as coatings, paints, and fire retardant materials.[13−20] The influence of curvature and confinement on polymer chain dynamics is thus of critical importance.

While there have been many attempts to characterize the immobilized polymer layer on nanoparticles, the current understanding of this underpinning quantity is poor. We use three examples from the current literature to illustrate this point. (i) Molecular dynamics simulations[3] show that the immobilized layer thickness does not change with particle size. However, these simulations only consider particle−polymer couples that interact through repulsive interactions. The relevance of these calculations to experiments, where attractions should play an important role, is unclear. (ii) Bogoslovov et al.[6] examined the segmental dynamics of polymers filled with 100 nm diameter silane-coated silica particles and found no evidence of an immobilized polymer layer. We make a geometric calculation assuming uniform particle dispersion for the face-to-face spacing, h. We define $h = V_{poly}/S_{Si}$, the ratio of the volume of polymer to silica surface area, and determine it from known inputs

$$\frac{V_{poly}}{S_{Si}} = \frac{\varphi_{poly}}{1-\varphi_{poly}}\frac{D}{6} \quad (1)$$

*Corresponding authors.

© 2010 American Chemical Society
Published on Web 03/02/2010

where φ_{poly} is the volume fraction of polymer (relative to polymer and particle), and D is the particle diameter. For their highest particle loading, $h \approx 43$ nm, at least an order-of-magnitude larger than the bound layer thickness (~5 nm on flat surfaces). We conjecture that these experiments, which are in the regime where property changes are within the error bars of the measurements, cannot reliably estimate the bound layer thickness. (iii) Sargsyan et al.[7] used smaller particles (10 nm in diameter) and higher particle loadings (up to 50% by weight) so that h would be < 10 nm if the particles were well dispersed. Unfortunately, these studies are hampered by the ubiquitous problem of poorly dispersed nanoparticles. Therefore, while there have been many studies that have attempted to determine the thickness of the bound polymer layer, they have been hampered by selection of simulation parameters and conditions or various experimental challenges.

Here we focus on this unresolved issue by achieving high loadings of well-dispersed isolated nanoparticles with attractive polymer-surface interactions. By using a suite of complementary experimental and theoretical tools, we characterize the immobilized polymer layer thickness on spherical nanoparticles and delineate its consequences on chain dynamics. We compare the behavior of poly(2-vinylpyridine) (P2VP) films cast on planar silica substrates (films as thin as 8 nm), which represents the ultimate limit of a large particle composite, to P2VP with well-dispersed $D = 15$ nm silica nanoparticles (D is the particle diameter), with surface-to-surface separations as low as 5 nm. Measurement of chain immobilization using positron annihilation lifetime spectroscopy (PALS) is supported by differential scanning calorimetry (DSC) and shows that the thickness of the bound layer goes from ~4 to 5 nm layer at planar surfaces to a ~1 nm thick layer near the highly curved silica particles. Dielectric relaxation spectroscopy (DRS) results show that the fragility of the P2VP in the nanocomposites is essentially unchanged, even for the highest particle loading, although the segmental dynamics is itself slowed down. While a systematic study of the dependence of the bound polymer layer thickness on particle size remains an outstanding challenge, this first study provides conclusive evidence that the bound polymer layer can been significantly smaller around nanoparticles than at chemically similar flat surfaces.

2. Systems Studied and Experimental Details

P2VP-40 ($M_w \approx 40$ kDa), P2VP-100 ($M_w \approx 100$ kDa), and P2VP-200 ($M_w \approx 200$ kDa) (Scientific Polymer Products), 2-Butanone (MEK), and pyridine (Sigma-Aldrich) were used as received. Irganox 1010 (antioxidant) was donated by Ciba, and colloidal silica in MEK (30% w/w) was donated by Nissan Chemicals.

We discuss the preparation of the nanocomposites in Section 3 below. For the preparation of P2VP-100 thin films, silicon (100) wafers were cut into 2.5×2.5 cm^2 squares and cleaned according to previously outlined procedures.[21] First, the wafers were soaked in an aqueous hydrogen peroxide and ammonium hydroxide solution to clean the surface of organic contaminants. Next, the surfaces were immersed in hydrofluoric acid (10% in deionized water), rinsed with deionized water, and blown-dry with nitrogen. Finally, the samples were placed in a UV-ozone oven for 30 min to grow a surface oxide layer (2 nm) and promote the formation of surface silanols.[21] P2VP-100 and Irganox 1010 (0.1 wt % relative to polymer only) were dissolved in chlorobenzene (at varying concentrations to control sample thickness) and filtered through 0.45 μm PTFE syringe filters. Solutions were spin-cast at 3000 rpm, and the samples were annealed at 160 °C for 48 h in vacuo to remove residual solvent and promote relaxation of the polymer chains.[22,23] Thicknesses for the glassy films at room temperature (~25 °C) were measured with a single-wavelength ellipsometer using the measured oxide layer thickness (2 nm). The error of the polymer film thickness measurements is approximately ±1 nm. Immediately prior to thin film PALS analysis, the films were heated to 180 °C and allowed to slowly cool to 25 °C.

Depth-profiling beam PALS[5,24,25] and bulk PALS[5,24,25] were performed according to previously established procedures. Thin films were analyzed using a variable energy, focused beam of positrons in high vacuum. By controlling the implantation energy of the positrons from 1 to 4 keV, we can control the mean positron implantation depth in the film from about 10 to 300 nm. With bulk PALS, a small amount of ^{22}Na radioactive source (~10 mCi) is sandwiched between two identical nanocomposite samples. The energetic β-decay positrons implant up to ~0.5 mm deep and hence probe the bulk of the sample.

Fourier transform infrared spectroscopy (FTIR) was performed on a Digilab/Biorad 7000 spectrometer with 2 cm^{-1} resolution and 64 scans. Samples were placed on 25 mm diameter × 2 mm thick NaCl windows for processing and analysis. Modulated DSC[26] was performed using an indium- (temperature) and sapphire- (heat capacity) calibrated TA Instruments Q100 in a nitrogen atmosphere. Approximately 10 mg of sample was placed in an aluminum sample pan and held at 190 °C for 5 min. These samples were then cooled at a rate of 2 °C/min, with a modulation amplitude of 1 °C and a modulation period of 60 s, to a final temperature of 30 °C. The TA Instruments software package, Universal Analysis 2000, was used to quantify the glass-transition temperature, T_g. The inflection-point in the transition of the total heat capacity from the rubbery state to the glassy state was interpreted as the T_g, and at least three samples were averaged at each state point.

DRS was performed on a Novocontrol α high-resolution dielectric analyzer that is equipped with heating/cooling controls, including Novocontrol's Novocool system. P2VP discs were placed on a dielectric sample cell 12 mm in diameter and covered by another sample cell of the same size. This sandwiched sample was placed between two electrodes, ensuring that no gaps were present. The frequency sweeps were conducted in the temperature range from 160 to 100 °C in 3 °C intervals and 100 to −40 °C in 10 °C intervals in the frequency range of 10^{-2} to 10^6 Hz. The first scan at 160 °C was repeated three times to ensure that the sample was thermally equilibrated during the analysis. Dielectric permittivity spectra were analyzed by fitting to the Havriliak−Negami and Cole−Cole functions, along with a conductivity contribution to obtain the relaxation times for the α and β relaxation processes, respectively.[27] At least three identically prepared samples were averaged at each temperature.

For TEM, samples were cut into ~50 nm slices using ultramicrotomy. For the analysis of the interparticle spacings, ultrasmall angle X-ray scattering (USAXS) was performed at beamline X10A at the National Synchrotron Light Source. The silica primary particle radius ($R_p = 7.5 \pm 2.2$ nm) was also determined using SAXS at X10A with a fit to a Gaussian-convoluted form factor.

3. Nanocomposite Design and Preparation

A critical question here is the optimal choice of particle size for this study. For guidance, we examine the predictions of self-consistent mean-field theory[28] for the thickness of the "bound" polymer layer. The 1D self-consistent mean-field theory of Scheutjens and Fleer was used to probe theoretically the adsorbed layer thickness as a function of particle radius.[29] Our calculations are for an isolated spherical nanoparticle in an infinite polymer matrix. Approximations for the effects of curvature have been previously outlined.[29] An incompressible cubic lattice was filled with chains of length 500, and the adsorbed layer thickness was determined by the root-mean-square thickness of chains containing at least one segment in contact with the surface normalized to the adsorbed layer thickness on a planar surface. As shown in Figure 1, the bound layer thickness reduces

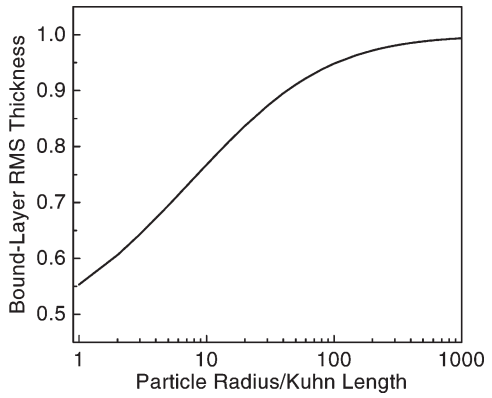

Figure 1. Predictions of mean-field theory for the rms thickness of the bound polymer layer. The bound polymer layer contains any chain with at least one segment in contact with the surface.

by a factor of ~2 when going from planar surfaces to small nanoparticles.

Our work (to be presented in Figure 8) shows that in the case of planar films we must use films thinner than ~20 nm before we can characterize the bound layer thickness outside error. For larger thickness, Figure 8 shows that the thin film data for the thermal expansion coefficient in the liquid phase are identical to the bulk within relatively large error bars. Given the theoretical prediction that the bound layer on small nanoparticles is a factor of 2 smaller than that on planar surfaces, it follows that the face-to-face separations in the case of nanoparticles must be 10 nm and thinner to yield sensible experimental results. This immediately suggests that the experiments of Bogoslovov, which used 100 nm particles and accessed face-to-face separations of 43 nm (and larger), are in the regime where errors dominate the experiments. Using eq 1 and a maximum nanoparticle volume fraction of 0.3, we thus have to use particles smaller than ~25 nm to satisfy experimental signal-to-noise requirements. Such small nanoparticles would combine the dual advantages of experimental ease and be in a size range where theory suggests that we can expect substantially decreased bound layer thicknesses relative to flat surfaces. In this range of thickness, there is a commercially available silica nanoparticle system with a particle diameter of 15 ± 4 nm, which is particularly appropriate. We employ these nanoparticles in our work.

In this context, it is crucial to have the ability to tune the dispersion of nanoparticles in a polymer matrix. This is a difficult challenge, even in the case of favorable polymer−particle interactions, because the activation energy required to break up a unit mass of "dry" particle clusters also scales as $1/R$.[30] Therefore, reducing particle size from 1 μm to 10 nm increases the energy requirement by a factor of 100! Numerous strategies have been implemented to facilitate the dispersion of nanoparticles within polymers, including the addition of surfactants,[1,31] in situ polymer-nanocomposite synthesis,[32] grafted nanoparticles,[33,34] spin-casting,[12] and rapid precipitation from solution.[35,36]

Inspired by these ideas, here we implement a novel dispersion strategy to explore properly the influence of the confining geometry on polymer chain immobilization. We prepared the nanocomposites by dissolving P2VP and Irganox 1010 (0.1% w/w relative to polymer only) in MEK. In a separate vial, the silica suspension was diluted with pyridine (33% v/v), and the solution was sonicated with a probe sonicator for 5 min. Pyridine plays a crucial role in properly dispersing the particles within the P2VP melt: in the absence of pyridine, P2VP strongly binds to the silica surfaces, even in the presence of MEK, and causes the P2VP to "crosslink" the silica. A silica-P2VP gel then precipitates out, causing poor particle dispersion in the resulting

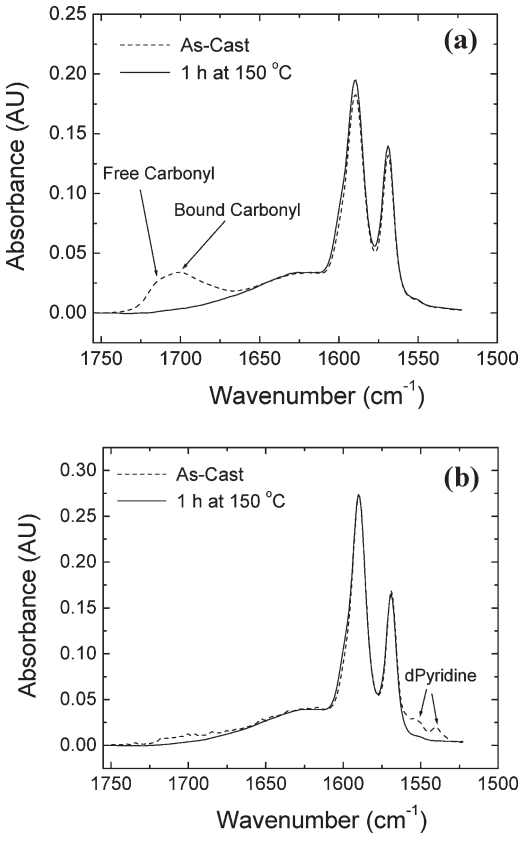

Figure 2. (a) FTIR spectra of the filled P2VP samples. No pyridine was added to the silica suspension for a P2VP/silica nanocomposite with 80 wt % silica. Note that the bound carbonyl from the MEK adsorbed to the silica nanoparticles. (b) Isotopically labeled (deuterated) pyridine (dPyridine) added to silica suspension for a P2VP/silica nanocomposite with 80 wt % silica. After 1 h at 150 C, all of the dPyridine was removed from the nanocomposite.

nanocomposite. The addition of the pyridine, which competitively hydrogen bonds with the silica surface, thereby preventing silica-P2VP gelation and precipitation, alleviates this problem. Various concentrations of the silica suspension were added to P2VP solutions, and the polymer/silica suspensions were vigorously shaken for 2 h, followed by 1 min of ultrasonication, poured into PTFE drying dishes, and allowed to sit overnight in a fume hood. The cast films were annealed in vacuo (~10^{-3} mm Hg) at 150 °C for 48 h and then compression-molded at 180 °C for 5 min into 12.7 mm diameter × 0.8 mm thick discs. The discs were subsequently annealed at 110 to 120 °C (depending on filler loading) in vacuo for 2 h to remove any stresses from compression molding.

FTIR was used to (i) confirm complete removal of the pyridine during nanocomposite annealing through the use of isotopically labeled (deuterated) pyridine to distinguish it from the P2VP spectrum and to (ii) quantify the strong hydrogen bonding interactions between the P2VP and silica (Figure 2). FTIR was also used to confirm no measurable polymer degradation under any conditions implemented here. Using a method reported previously, we estimated the hydrogen-bonded fraction after Gaussian fits to the pyridyl intensities at 1598 and 1590 cm^{-1} using the equation

$$\text{H-bonds/nm}^2 = \frac{I_{1598}}{I_{1598} + \alpha I_{1590}} \frac{N_A \rho_{poly} V_{poly}}{M_{w_{seg}} S_{Si}} \qquad (2)$$

where α is the ratio of absorption coefficients ($\alpha \approx 1$),[37] N_A is the Avogadro constant (6.02×10^{23} mol^{-1}), ρ_{poly} is the polymer

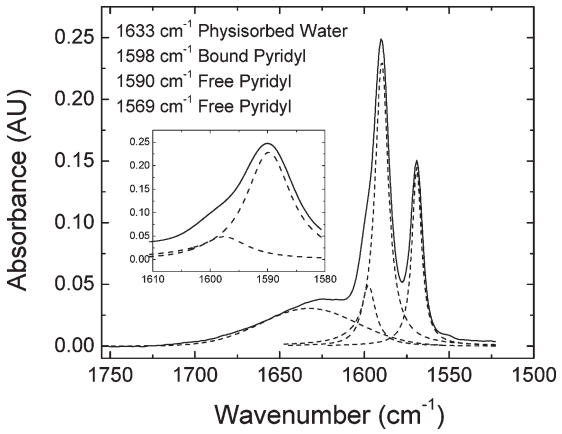

Figure 3. FTIR of filled P2VP samples. Sample with dPyridine added to silica suspension after 24 h at 150 °C. The inset shows an expansion around the bands pertinent for determination of the degree of hydrogen bonding at 1598 (bound) and 1590 (free) cm^{-1}. Approximately 1.5 hydrogen bonds/nm^2 were determined from a fit to the data using eq 1.

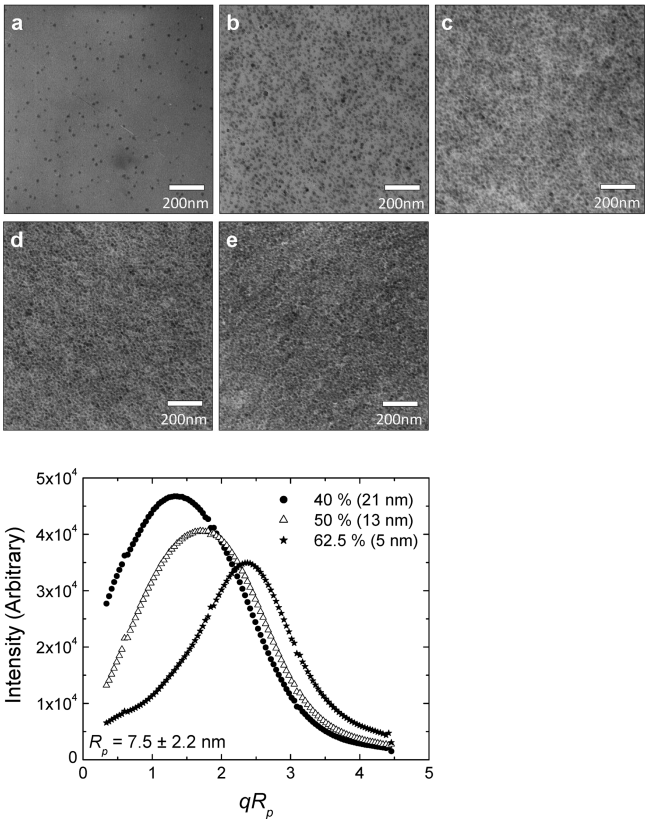

Figure 4. TEM images for P2VP nanocomposites with (a) 1, (b) 20, (c) 40, (d) 50, and (e) 62.5 wt % silica. Also shown are the USAXS results for 40, 50, and 62.5 wt % silica.

density (~1.05 g/cm^3), $M_{w_{seg}}$ is the segmental molecular weight, and (V_{poly}/S_{Si}) is defined following eq 1.

The broad infrared band at 1633 cm^{-1}, which was also fit to a Gaussian line shape, is associated with physisorbed water on the surface of silica.[38] Results show ~1.5 hydrogen bonds/nm^2 formed between the P2VP and the silica (Figure 3). This translates to a P2VP/silica adhesive energy (i.e., work of adhesion) of approximately −350 mJ/m^2.[39] Compared with the work of adhesion for pure P2VP (about −70 mJ/m^2),[40] this is a very attractive interface.

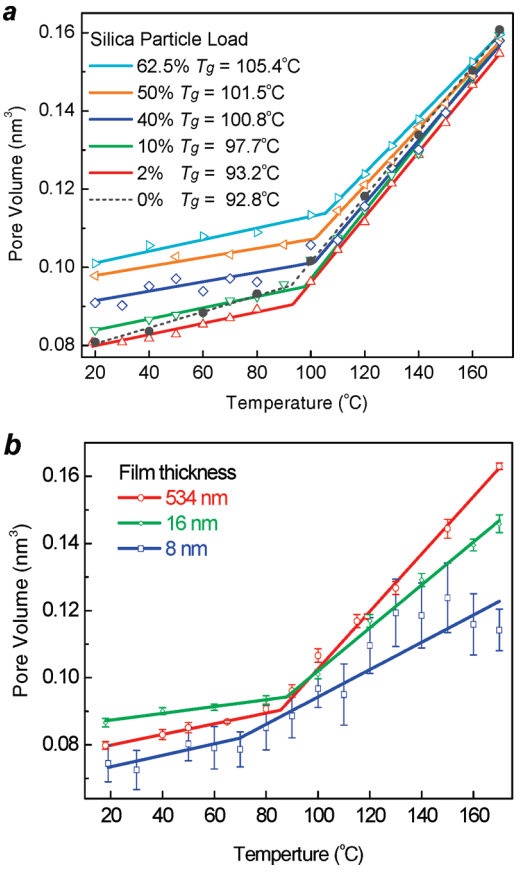

Figure 5. (a) PALS-determined mean "free" volume for nanocomposite films with various loadings of silica. (b) Corresponding data for three thin films on silica surfaces.

4. Results and Discussion

For characterization of particle dispersion, we used the complementary techniques of transmission electron microscopy (TEM) and small-angle and ultra-small-angle X-ray scattering (SAXS/USAXS) (Figure 4). Whereas the TEM results appear to suggest that good dispersion is achieved in all cases, it is hard to interpret these findings especially for the high particle loadings (> 20 wt % silica), where the finite thickness of the TEM slices (~50 nm) could cloud the issue because of the 2D projection of a 3D sample. The USAXS data at low loadings only show a peak corresponding to the form factor of the silica nanoparticles. Analysis of these results suggest that the particles are 15 ± 4 nm in diameter, which is in good agreement with manufacturer specifications. At higher loadings (Figure 4f), the data show pseudo-Bragg peaks corresponding to interparticle "diffraction." Analysis of the results, along with the measured particle diameters, yields the average surface-to-surface distances of the particles in the highly filled nanocomposites. At 62.5 wt % silica loading, results show a 5 nm average separation, a result that is nicely bracketed by two geometrical estimates: (i) V_{poly}/S_{Si} = 6 nm, where V_{poly} is the polymer volume and S_{Si} is the silica surface area, and (ii) $D \times [\phi_{polymer}^{-1/3} - 1] = 4.2$ nm, both of which assume uniform particle dispersion. We are thus confident that the particles are well dispersed in the polymer matrix, even at the highest loadings.

We next examine free volume void sizes determined by positron annihilation lifetime spectroscopy (bulk-PALS for nanocomposites and beam-PALS for thin P2VP films on silica substrates) for evidence of an immobilized interface layer as the sample temperature is stepped up (or down; no difference observed in cooling) between room temperature and 170 °C. Figure 5a shows the mean "free" volume void sizes, deduced

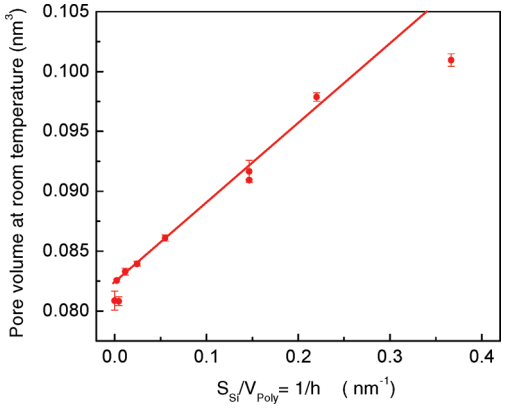

Figure 6. Polymer pore volume measured in the nanocomposite glassy phase (at 20 °C) shows nominally linearly increasing strain with the ratio of the silica surface to the polymer volume, S_{Si}/V_{poly}, (which is also equal to the inverse of the effective polymer layer thickness, h, as the x axis).

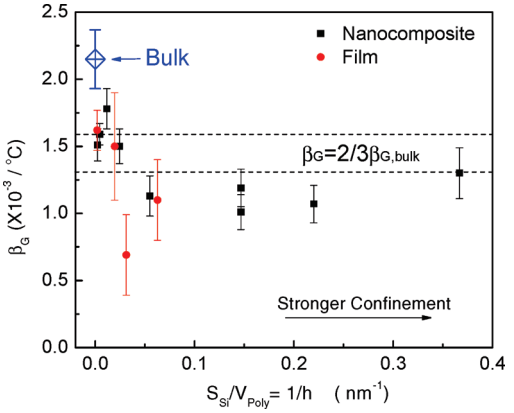

Figure 7. The fitted volume expansion coefficients, β_G, in the glassy phase plotted as a function of the S_{Si}/V_{poly}, which is also proportional to the inverse of the film thickness (or the nanocomposite effective thickness), h. For a polymer confined by surface adhesion, the expected value of β_G is ~$2/3\beta_{G,bulk}$, when Poisson's ratio is ~1/3. The two dashed lines represent the expected range for β_G given the error in the measured bulk coefficient. The data are in agreement with this expectation with no differentiation between films and nanocomposites. It does suggest that the immobilized layer may not have truly zero thermal expansion but is still reduced a factor of 10 from the bulk rubber phase coefficient.

directly from the fitted Ps lifetimes (τ = 1.8 to 2.8 ns) using the well accepted Tao−Eldrup relationship[41,42] as a function of temperature for some representative nanocomposite samples. Each point is an average of several runs, including both heating and cooling cycles. Figure 5b shows the corresponding data for three (the two thinnest and the thickest films) of the five thin film samples. These temperature scans allow us to fit for the usual apparent T_g and volume expansion coefficients in the glassy and rubbery states; we begin by discussing the PALS-deduced void volume, which offers conclusive evidence of a "bound" polymer layer.

PALS (especially bulk-PALS) can be thought of as a highly sensitive form of absolute polymer dilatometry; the average free volume void size is quantitatively determined, regardless of silica loading, and the expansion coefficients are 10−20 times the total volume expansion coefficient because PALS is sensitive only to the free volume of the polymer. (Note the factor of two increase in void volume on heating to 170 °C in Figure 5.) Therefore, the most noticeable feature in Figure 5a is the silica concentration-dependent volume strain in the nanocomposites' glassy polymer free volume that is relatively absent from the thin film results (including data not presented in Figure 5b for clarity). To probe the source of stress, which produces the increasing strain with silica concentration, the void volume measured at room temperature is plotted in Figure 6 as a function of the calculated silica surface to polymer volume ratio (S_{Si}/V_{poly} = $1/h$). The linear dependence immediately emphasizes that this "strain" is driven by nanoparticle surfaces, thus implicating an effectively immobilized "bound" layer in this context. Furthermore, we speculate that interparticle surface attachment of the polymer molecules prevents the normal relaxation of the polymer. This last statement is given credence by the fact that the thin films supported on silica do not display any such clearly defined volume strain in the glass phase; we attribute this to the inability of a single silica substrate to have interparticle attachments, as would be the case for a doubly supported film (the planar model analogy for the composites). Despite this difference in absolute free volume between the films and the nanocomposites, the measured relative (total) volume expansion coefficients are all consistent with that expected from simple polymer confinement by surface adhesion and with a typical value of 0.33 for Poisson's ratio, $\beta_G \approx 2/3\beta_{G,bulk}$ (Figure 7). Given the small thermal expansion of the glass phase and the presence of large volume strains, we shift our search for quantitative evidence of an immobilized polymer layer to the rubber phase above T_g, where relative volume expansion is an order of magnitude larger and volume strains are not an issue.

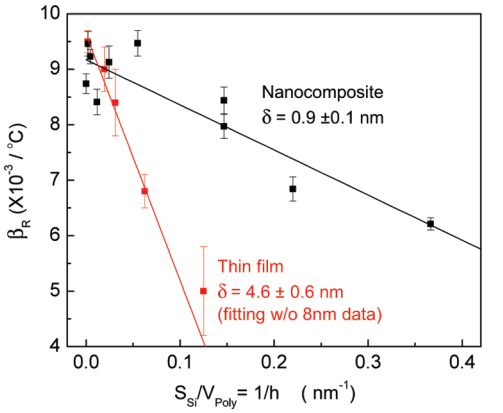

Figure 8. Linear fits of the rubber phase volume expansion coefficients, β_R, indicate consistency with the two-layer model but with very different fitted values of the nonexpanding layer thicknesses, δ: δ = 4.6 ± 0.6 nm for thin films and δ = 0.9 ± 0.1 nm for nanocomposites. We did not include the systematically less reliable 8 nm thin film data point in this fit (even though inclusion of it yields a very similar value of δ = 4.3 nm).

To quantify the "immobilized" layer of polymer in the rubber phase, we use a simple two-layer model of a nonexpanding film of thickness, δ, in contact with material with the bulk rubber expansion coefficient, $\beta_R(\infty)$. Then, we expect the fitted volume expansion coefficient for a film of thickness, h, or a nanocomposite of effective thickness, h = $(S_{Si}/V_{poly})^{-1}$, to follow

$$\beta_R(h) = \beta_R(\infty)\left[1 - \frac{\delta}{h}\right]$$

In Figure 8, we plot the fitted $\beta_R(h)$ versus $1/h$ = (S_{Si}/V_{poly}) for both the nanocomposites and the planar thin films. The decrease in $\beta_R(h)$ is consistent with the linear drop expected from the two-layer model. Notably, the fitted values of δ are very different: 4.6 ± 0.6 nm for the planar films, in good agreement with literature estimates, but only 0.9 ± 0.1 nm for the nanocomposites. This very small value of δ for the curved particle surface is corroborated by DSC results below.

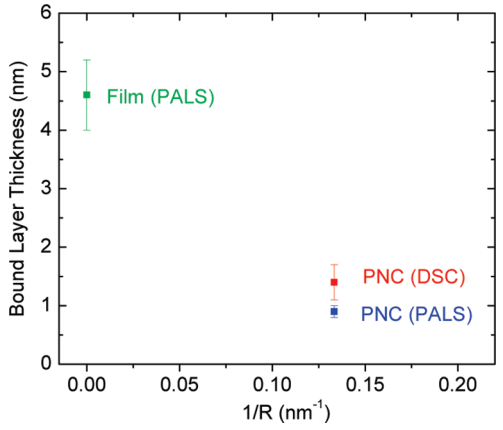

Figure 9. Summary of the bound layer thicknesses deduced by PALS for both the films and the PNCs and, for comparison, by DSC for the PNCs. The parameter R is the effective radius of curvature for the silica surface in contact with the P2VP polymer.

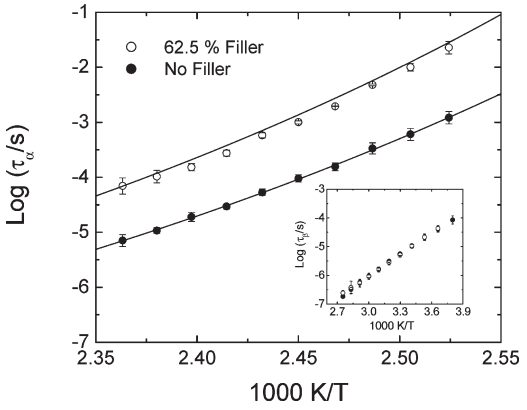

Figure 10. Dielectric relaxation spectroscopy results for the α-relaxation times (τ_α) for pure P2VP and P2VP filled with 62.5 wt % silica nanoparticles. The inset shows the measured β-relaxation times (τ_β) for the glassy systems. The α-relaxation times were determined with a fit to the Havriliak−Negami equation, whereas the β-relaxation times were determined with a fit to the Cole−Cole equation.

Our analysis of the DSC results closely follows the published protocol of Sargysan et al. and is therefore not repeated here.[7] Although the errors are much greater for the bound layer thickness determined following DSC, δ_{DSC} (about ±0.6 nm per sample), we deduce $\delta_{DSC} = 1.4 \pm 0.3$ nm by combining all of the data for the three different molecular weights (there was no discernible trend with M_w). These three results, summarized in Figure 9, clearly demonstrate that the thickness of the immobilized polymer layer in the rubber phase is significantly reduced going from a flat surface to a nanoparticle with diameter of 15 nm.

To this point, we have examined essentially equilibrium quantities in the rubber phase to determine the thickness of the bound layer at the nanoparticle surfaces. We now examine the dynamic consequences of this bound layer. Figure 10 shows the α and β relaxation times (τ_α and τ_β, respectively) for the pure and filled P2VP, as determined by DRS. We consider the two extreme cases of the pure polymer and one filled with 62.5 wt % silica. The τ_α curves from the two samples are parallel to each other, with the filled system corresponding to slower relaxation times. Fitting the data to the Vogel−Fulcher−Tammann form,[27] $\tau_\alpha = \tau_0 \exp[-(BT_0)/(T - T_0)]$, where τ_0 is a prefactor, B is a measure of fragility, and T_0 is the Vogel temperature, yields that the fragility is essentially unchanged, whereas T_0 has a very small shift, as will be further explained below.[43−46] This is similar to previously

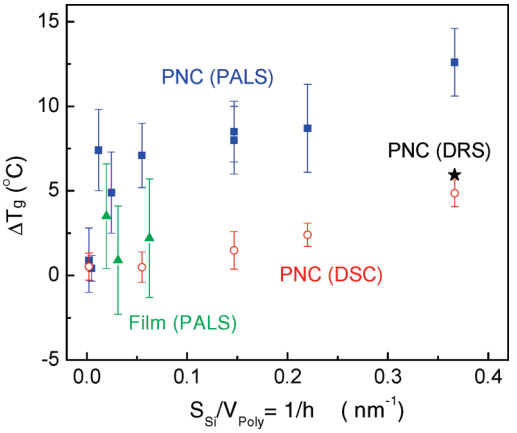

Figure 11. Thin film and nanocomposite (NCP) results for the apparent glass-transition temperature as a function of the inverse of the effective film thickness using DSC, PALS, and DRS.

reported results for P2VP in planar films, where the relaxation mechanism of the mobile chains is still highly cooperative motion. The local, or noncooperative, β-process also showed negligible changes in the Arrhenius activation energy (~50 kJ/mol) and actual relaxation times for the glassy systems. Therefore, confinement plays a very minor role on the temperature dependence of segmental dynamics.

For the sake of completeness, we plot the apparent nanocomposite and thin film T_g data in Figure 11. We find that ΔT_g, the deviation of the T_g from its bulk value, for the nanocomposites from all three measurement tools is positive and increases with increased particle loading. While the DSC and the dielectric spectroscopy (determined by the difference in Vogel temperatures) measurements are internally consistent, the T_g changes determined by PALS for the nanocomposites are somewhat larger. These results are not really surprising in light of multiple reports in the literature that ΔT_g is measurement tool and scan-rate-dependent and can sometimes even have different signs.[47] Regardless, these T_g changes are much smaller (typically an order of magnitude smaller) than the results previously presented by Torkelson and his coworkers on thin films of P2VP-silica nanocomposites.[12] We attribute this discrepancy to the fact that Torkelson et al. used thin films of nanocomposites;[48] bulk nanocomposite samples gave very small ΔT_g values, in agreement with our findings. In this context, we note that our derivation of immobile layer thicknesses is not dependent on these apparent values of T_g.

5. Relationship to Previous Works

There are several[12] previous works whose results are worth discussing in the context of the current work. First, our conclusion that nanoparticles offer significantly fewer confinement effects than flat surfaces appears, at first sight, to contradict our previous conclusions of a quantitative equivalence between nanocomposites and thin polymer films.[14] It is important to emphasize that the previous results were in the case of a nonwetting particle interface where such bound-layer effects play essentially no role. Therefore, we do not believe that our current work has much bearing on the quantitative equivalence proposed in that previous work. More pertinent might be the results of Torkelson and coworkers,[12] who suggested that the equivalence between thin films and nanocomposites might be qualitative at best. As we have discussed above, the T_g shifts measured by Torkelson et al. are much larger than those we find for both the thin films and the nanocomposites. In the present case, both the flat surfaces and the nanocomposites show practically no changes in T_g with decreasing film thickness. A similar lack of T_g shifts has

been reported for thin films floating on ionic liquids.[48] Thus, at this time, we do not believe that there is conclusive data that support or invalidate the equivalence of T_g behavior between thin films and nanocomposites in the case of attractive polymer−particle interfaces.

6. Concluding Remarks

Our results clearly emphasize that small nanoparticles, when well-dispersed within a polymer matrix, provide significantly fewer confinement effects when compared with flat surfaces with the same chemistry. This is evident with a decrease in immobilized layer thicknesses, as predicted theoretically and confirmed experimentally using DSC and PALS. However, similar to previously reported results for P2VP on flat surfaces, T_g changes are small, and the molecular dynamics do not undergo any significant changes in cooperative motion relative to bulk P2VP, as determined using DRS. As noted in the introductory paragraph, these results have crucial implications for the unusual nanoparticle size dependence of macroscale nanocomposite properties, including a postulated maximum in the mechanical reinforcement.[8] We emphasize that experiments on larger particle sizes would have been particularly appropriate because this would have allowed us to delineate the size dependence of the bound polymer layer; however, as discussed extensively, we are restricted to particle sizes < 20 nm for currently available experimental techniques to yield meaningful results. There is, of course, the possibility that we can study nanoparticles with bound layers alone (without any matrix polymer), a protocol that has been very successfully used by Blum and his coworkers to characterize the segmental dynamics and T_g of these adsorbed layers.[49] Unfortunately, these previous workers have shown that the resulting polymer layer's properties (such as T_g and bound layer thickness) are very dependent on preparation conditions, including any annealing protocol that is followed. The intermediate range of particle sizes (50−500 nm), which will allow us to map the size dependence of the bound layer, thus remains outside the purview of any currently available experimental protocol. This remains an open challenge in this field.

Acknowledgment. The Michigan positron group gratefully acknowledges the research assistance of undergraduates Ross Smith, David Welch, Maeve Manion-Fischer, and Alex Gidley.

References and Notes

(1) Balazs, A. C.; Emrick, T.; Russell, T. P. *Science* **2006**, *314*, 1107–1110.
(2) Bohning, M.; Goering, H.; Hao, N.; Mach, R.; Schonhals, A. *Polym. Adv. Technol.* **2005**, *16*, 262–268.
(3) Brown, A.; Marcadon, V.; Mele, P.; Alberola, N. D. *Macromolecules* **2008**, *41*, 1499–1511.
(4) O'Shaughnessy, B.; Vavylonis, D. *Phys. Rev. Lett.* **2003**, *90*, 056103.
(5) DeMaggio, G. B.; Frieze, W. E.; Gidley, D. W.; Zhu, M.; Hristov, H. A.; Yee, A. F. *Phys. Rev. Lett.* **1997**, *78*, 1524–1527.
(6) Bogoslovov, R. B.; Roland, C. M.; Ellis, A. R.; Randall, A. M.; Robertson, C. G. *Macromolecules* **2008**, *41*, 1289–1296.
(7) Sargsyan, A.; Tonoyan, A.; Davtyan, S.; Schick, C. *Eur. Polym. J.* **2007**, *43*, 3113–3127.
(8) Edwards, D. C. *J. Mater. Sci.* **1990**, *25*, 4175–4185.
(9) Serghei, A.; Tress, M.; Kremer, F. *Macromolecules* **2006**, *39*, 9385–9387.
(10) Napolitano, S.; Lupascu, V.; Wübbenhorst, M. *Macromolecules* **2008**, *41*, 1061–1063.
(11) Shin, K.; Obukhov, S.; Chen, J. T.; Huh, J.; Hwang, Y.; Mok, S.; Dobriyal, P.; Thiyagarajan, P.; Russell, T. P. *Nat. Mater.* **2007**, *6*, 961–965.
(12) Rittigstein, P.; Priestley, R. D.; Broadbelt, L. J.; Torkelson, J. M. *Nat. Mater.* **2007**, *6*, 278–282.
(13) Alexandre, M.; Dubois, P. *Mater. Sci. Eng., R* **2000**, *28*, 1–63.
(14) Bansal, A.; Yang, H. C.; Li, C. Z.; Cho, K. W.; Benicewicz, B. C.; Kumar, S. K.; Schadler, L. S. *Nat. Mater.* **2005**, *4*, 693–698.
(15) Bockstaller, M. R.; Mickiewicz, R. A.; Thomas, E. L. *Adv. Mater.* **2005**, *17*, 1331–1349.
(16) Giannelis, E. P.; Krishnamoorti, R.; Manias, E. Polymer-Silicate Nanocomposites: Model Systems for Confined Polymers and Polymer Brushes. In *Polymers in Confined Environments*; Springer: New York, 1999; Vol. *138*, pp 107−147.
(17) Gilman, J. W.; Kashiwagi, T.; Lichtenhan, J. D. *SAMPE J.* **1997**, *33*, 40–46.
(18) Hule, R. A.; Pochan, D. J. *MRS Bull.* **2007**, *32*, 354–358.
(19) Krishnamoorti, R. *MRS Bull.* **2007**, *32*, 341–347.
(20) Krishnamoorti, R.; Vaia, R. A. *J. Polym. Sci., Part B: Polym. Phys.* **2007**, *45*, 3252–3256.
(21) Frantz, P.; Granick, S. *Langmuir* **1992**, *8*, 1176–1182.
(22) Hub, C.; Harton, S. E.; Hunt, M. A.; Fink, R.; Ade, H. *J. Polym. Sci., Part B: Polym. Phys.* **2007**, *45*, 2270–2276.
(23) Sen, S.; Xie, Y.; Bansal, A.; Yang, H.; Cho, K.; Schadler, L. S.; Kumar, S. K. *Eur. Phys. J.* **2007**, *141*, 161–165.
(24) Xie, L.; Demaggio, G. B.; Frieze, W. E.; Devries, J.; Gidley, D. W.; Hristov, H. A.; Yee, A. F. *Phys. Rev. Lett.* **1995**, *74*, 4947–4950.
(25) Hristov, H. A.; Bolan, B.; Yee, A. F.; Xie, L.; Gidley, D. W. *Macromolecules* **1996**, *29*, 8507–8516.
(26) Wunderlich, B.; Jin, Y. M.; Boller, A. *Thermochim. Acta* **1994**, *238*, 277–293.
(27) Papadopoulos, P.; Peristeraki, D.; Floudas, G.; Koutalas, G.; Hadjichristidis, N. *Macromolecules* **2004**, *37*, 8116–8122.
(28) Fleer, G. J.; Stuart, M. A. C.; Scheutjens, J. M. H. M.; Cosgrove, T.; Vincent, B. *Polymers at Interfaces*; Chapman & Hall: New York, 1993.
(29) Fleer, G. J.; Stuart, M. A. C.; Scheutjens, J. M. H.; Cosgrove, T.; Vincent, B. *Polymers at Interfaces*; Chapman & Hall: New York, 1993.
(30) Alter, H. *J. Appl. Polym. Sci.* **1965**, *9*, 1525–1531.
(31) Harton, S. E.; Kumar, S. K. *J. Polym. Sci., Part B: Polym. Phys.* **2008**, *46*, 351–358.
(32) Narayanan, R. A.; Thiyagarajan, P.; Lewis, S.; Bansal, A.; Schadler, L. S.; Lurio, L. B. *Phys. Rev. Lett.* **2006**, *97*, 075505.
(33) Bansal, A.; Yang, H. C.; Li, C. Z.; Benicewicz, R. C.; Kumar, S. K.; Schadler, L. S. *J. Polym. Sci., Part B: Polym. Phys.* **2006**, *44*, 2944–2950.
(34) Akcora, P.; Liu, H.; Kumar, S. K.; Moll, J.; Li, Y.; Benicewicz, B. C.; Schadler, L. S.; Acehin, D.; Panagiotopoulos, A. Z.; Pryamitsyn, V.; Ganesan, V.; Ilavsky, J.; Thiyagarajan, P.; Colby, R. H.; Douglas, J. F. *Nat. Mater.* **2009**, *8*, 354–359.
(35) Mackay, M. E.; Dao, T. T.; Tuteja, A.; Ho, D. L.; Van Horn, B.; Kim, H. C.; Hawker, C. J. *Nat. Mater.* **2003**, *2*, 762–766.
(36) Tuteja, A.; Mackay, M. E.; Narayanan, S.; Asokan, S.; Wong, M. S. *Nano Lett.* **2007**, *7*, 1276–1281.
(37) Lee, J. Y.; Painter, P. C.; Coleman, M. M. *Macromolecules* **1988**, *21*, 954–960.
(38) Basila, M. R. *J. Phys. Chem.* **1962**, *66*, 2223–2228.
(39) Coleman, M. M.; Graf, J. F.; Painter, P. C. *Specific Interactions and the Miscibility of Polymer Blends*; Technomic: Lancaster, PA, 1991.
(40) Sauer, B. B.; Dee, G. T. *Macromolecules* **2002**, *35*, 7024–7030.
(41) Tao, S. J. *J. Chem. Phys.* **1972**, *56*, 5499–5510.
(42) Eldrup, M.; Lightbody, D.; Sherwood, J. N. *Chem. Phys.* **1981**, *63*, 51–58.
(43) Labahn, D.; Mix, R.; Schönhals, A. *Phys. Rev. E* **2009**, *79*, 011801.
(44) Fukao, K.; Miyamoto, Y. *Phys. Rev. E* **2001**, *64*, 011803.
(45) Napolitano, S.; Prevosto, D.; Lucchesi, M.; Pingue, P.; D'Acunto, M.; Rolla, P. *Langmuir* **2007**, *23*, 2103–2109.
(46) Lupascu, V.; Picken, S. J.; Wubbenhorst, M. *J. Non-Cryst. Solids* **2006**, *352*, 5594–5600.
(47) Soles, C. L.; Douglas, J. F.; Wu, W. L.; Peng, H. G.; Gidley, D. W. *Macromolecules* **2004**, *37*, 2890–2900.
(48) Lu, H. Y.; Chen, W.; Russell, T. P. *Macromolecules* **2009**, *42*, 9111–9117.
(49) Lin, W. Y.; Blum, F. D. *Macromolecules* **1997**, *30*, 5331–5338.